Supplemental information

Scientific assessment of background ozone over the U.S.: Implications for air quality management

Daniel A. Jaffe[1,*], Owen R. Cooper[2,3], Arlene M. Fiore[4], Barron H. Henderson[5], Gail S. Tonnesen[6], Armistead G. Russell[7], Daven K. Henze[8], Andrew O. Langford[3], Meiyun Lin[9], and Tom Moore[10]

[1]University of Washington, School of Science, Technology, Engineering and Mathematics, Bothell, Washington, United States; and Department of Atmospheric Science, University of Washington, Seattle, Washington, United States
[2]University of Colorado, Cooperative Institute for Research in Environmental Sciences, University of Colorado, Boulder, Colorado, United States
[3] NOAA Earth System Research Laboratory, Chemical Sciences Division. Boulder, Colorado, United States
[4] Department of Earth and Environmental Sciences and Lamont-Doherty Earth Observatory of Columbia University, New York, New York, United States
[5]U.S. EPA, Research Triangle Park, North Carolina, United States
[6]U.S. EPA, Region VIII, Denver, Colorado, United States
[7]Georgia Institute of Technology, School of Civil and Environmental Engineering, Atlanta, Georgia, United States
[8]University of Colorado, Department of Mechanical Engineering, Boulder, Colorado, United States
[9]NOAA Geophysical Fluid Dynamics Laboratory, Princeton, New Jersey, United States
[10]Western States Air Resources (WESTAR) Council and Western Regional Air Partnership (WRAP), Fort Collins, Colorado, United States

[*]Corresponding author's email: djaffe@uw.edu

List of Contents:

Observations are April-September, 2000-2014. Vector colors indicate the p-values on the linear trend for each site: Blues indicate negative trends, oranges indicate positive trends, and green indicates weak or no trend; lower p-values have greater color saturation. Figure provided by the Tropospheric Ozone Assessment Report (Schultz et al., 2017). See Section 5 in main paper.

Figure S2. Annual 4th highest MDA8 O_3 for one site in each urban area.

The AQS ID numbers are given in Table S3. Data shown include any exceptional event days that may have been excluded from the O_3 design value calculation. See Section 5 in main paper.

Table S3. Linear trends and t-test results comparing 2000-2017 4th highest annual MDA8 values in 9 representative urban areas[a]

Supplementary Note 3. EPA and WAQS modeling platforms

Figure S3. Observed and modeled MDA8 O_3 for Rocky Mountain National Park (RMNP) monitor.

Observed (black line) and modeled MDA8 O_3 (EPA model, top of dark grey) with USB O_3 contributions from EPA model (top of light grey) and WAQS model (dashed green line) for the RMNP monitor. For four simulation segments, the values below the axis for both models give the mean bias (MB), correlation (r) of total prediction with observations (TOT), correlation of local contribution with observations (LC), and correlation of USB O_3 contribution with observations (USBO). See Section 6 in main paper.

Table S4. Correlation matrix for O_3 observations (OBS), predictions (Mod), and contributions at Chatfield[a]

Supplementary Note 4. Rationale for excluding stratospheric intrusion days in analysis

Supplementary references

Supplementary acknowledgements

Table S1. Model estimates for background ozone (O_3) (multiple definitions)[a]

Study; Model (horizontal resolution)	Study period; Metric	Background: Seasonal average values (ppb) *(High events)*	Approach/Notes
McDonald-Buller et al. (2011)[b], based on Zhang et al. (2011); GC[c] (½°x⅔°)	Mar-Aug 2006-2008; MDA8	NAB[d]: 39-44 (spring); 35-45 (summer); low-altitude 27±8; high-altitude 40±7 *(51-59, 4th highest)*	Zero-out
Emery et al. (2012); CAMx (12 km^2), GC boundary conditions	Mar-Aug 2006; MDA8	NAB: 25-50; 20-45 in GC (*35-100, 4th highest; 65 maximum without fires; 55 maximum in GC)*	Zero-out
Lin et al. (2012a); GFDL AM3 (~50km^2)	Apr-Jun 2010; MDA8	NAB: 15 western U.S. high-altitude sites 50±11 (*55±11, days when observed exceeds 60)*	Zero-out, bias corrected[e]
Huang et al. (2013); STEM (60x60	Jun-Jul 2008;	Transported background: MDA8 30-35 EPA Regions 9 and	Extrapolate adjoint

km^2)	MDA8 & W126	10; W126 10-17 ppm-h R9 & 3-4 ppm-h R10	sensitivities and bias-correct
Lapina et al. (2014); GC (2°x2.5°), AM3 (c48; ~200x200 km^2), and STEM (60x60 km^2)	May-Jul 2010; daytime O_3 & W126	NAB daytime O_3: multi-model spatial range of 18.3-41.6, US mean 56-67%, Intermountain West mean 64-78%; NAB W126: mostly < 3ppm hr, U.S.-wide mean 4-12%, <6 % in East, <35% in West	Zero-out
Dolwick et al. (2015); CMAQ, CAMx (12km^2)	Apr-Oct 2007; MDA8	USB[d] and USB[f]: Intermountain West 40-45, bias-corrected[g], seasonal mean; Pacific Coast 25-35 *(highest 10% of days in a season: >70-80%; western U.S. rural sites; >40-60%, western U.S. urban sites)*	Zero-out in CMAQ, source apportionment in CAMx
Fiore et al. (2014); GC (½°x⅔°)	Mar-Aug 2006; MDA8	NAB: western U.S. high-altitude sites ~40-50 (spring), ~25-40 (summer); eastern U.S. ~20-30 (summer)	Zero-out
Fiore et al. (2014); GFDL AM3 (2°x2°)	1981-2007 average	NAB:15-50, highest in western U.S. and in spring	Zero-out
Lefohn et al. (2014); GC/CAMx (12x12km^2)	2006	OSAT[f]-derived emissions-influenced background: *(can be >70% at high-elevation western U.S. sites)*	Source apportionment
Huang et al. (2015); GC (assimilated TES O_3)/STEM (assimilated OMI NO_2) (12×12 km^2)	Jun-Jul 2008; MDA8	USB[h]: Spatial range over CA and NV 35-65, domain mean of 48, 77% total	Zero-out within domain (CA and NV)
Lin et al. (2015); GFDL AM3 (c48; ~200x200 km^2)	1990-2012; MDA8	NAB over western U.S. Apr-May: 40-50 *(50-75 for observed O_3> 65)*; NAB over western U.S. Jul-Aug: 20	Zero-out
Dunker et al. (2017); CAMx /GC	March-Sep 2010; MDA8	USB[i] in 12 cities: (*ranges from 30.0 for Boston to 60.3 for Denver, and 42 for Boston to 64.8 for Denver, on 10 highest global background O_3 days)*	Path-integral method
Lin et al. (2017)[j]; GFDL AM3 (c48; ~200x200 km^2)	1980-2014; MDA8	Changes in western U.S. NAB from 1980s to 2000s: 6.3±1.9 (spring); 4.2±2.0 (summer)	Zero-out
Nopmongcol et al. (2016)[j]; CAMx /GC	1970-2020; 4th highest MDA8	USB: range increased from 40-55 to 45-60	Zero-out
Wild et al. (2012)[j]; 14 global models (1°x1° to 5°x5°)	1960-1990; annual mean	NAB: increased 0.67/decade, leveling off by 2000	Parameterization based on continental-average O_3 responses to 20% reductions in anthropogenic emissions

[a]Table is adapted and updated from Fiore et al. (2014) and focuses on work since the McDonald-Buller (2011) review. See Section 4 in main paper.
[b]References within this work include a comparison of Zhang et al. (2011) to earlier work.
[c]GC: GEOS-Chem.
[d]North American background (NAB) or U.S. background (USB), defined as the O_3 mole fractions sampled from the lowest (surface) model layer in a simulation with North American or U.S., respectively, anthropogenic emissions within the domain set to zero. Studies differ in their domain boundaries and also their treatments of fertilizer, shipping, agricultural waste burning and aircraft emissions.
[e]At sites where AM3 overestimates the observed MDA8 O_3 level, the bias is assumed to be caused entirely by excessive background.
[f]The Ozone Source Apportionment Technology (OSAT) in CAMx is designed to attribute O_3 formation to precursors tagged by source. When precursors come from multiple sources, O_3 is assigned to the source associated with the limiting chemical precursor (NO_x or VOC), which is identified based on an empirical threshold of radical termination pathways (i.e., if $P(H_2O_2)/P(HNO_3) > 0.35$ then NO_x, otherwise VOC).
[g]Bias-correction was calculated by taking the daily model calculated USB/Base MDA8 O_3 fractions and multiplying it by the daily MDA8 bias at each monitoring location. This product is then subtracted from the original USB[d] (zero-out) or USB[f] (source apportionment) estimate.
[h]Huang et al. (2015) zero-out anthropogenic emissions within the STEM domain (CA and NV) only so this estimate may include some O_3 produced from U.S. anthropogenic emissions that is transported through the boundary conditions.
[i]Calculated as Base – U.S. anthro columns of Table 3 (Dunker et al., 2017) for the base (T10Base) and high-background (T10Bkgd) days, which excludes a small (<0.5 ppb) anthropogenic contribution to the top boundary condition.
[j]This study looked at long-term O_3 trends.

Table S2. Model estimates for non-controllable ozone (O_3) sources (NCOS)[a]

Study; Model (horizontal resolution)	Study period; Metric	Non-controllable ozone source (NCOS): Mean estimate (ppb)[b] *(Events)*	Approach/Notes
McDonald-Buller et al., 2011[c], based on Zhang et al. (2011); GC[d] (½°x⅔°)	Mar-Aug 2006-2008; MDA8	Natural: 18±6 (low altitude), 27±6 (high altitude) *(34-45, 4th highest).* CH_4+ICT: 13-16 (spring) 11-13 (summer), 13 (high altitude), 9 (low altitude)	Zero-out
Mueller and Mallard (2011); CMAQ, GC boundary conditions (36 km^2)	2002; MDA8	Fires: *(30-50 western U.S.)* Lightning: *(10-30 southern U.S.)*	Zero-out
Brown-Steiner and Hess (2011); CAM-Chem	2001-2005; seasonal means	Asian: western U.S. 3.36 ± 1.3 (spring), 1.36 ± 0.7 (summer); central U.S. 1.66 ± 0.5 (spring), 0.70 ± 0.3 (summer); eastern U.S. 0.56 ± 0.3 (spring), 0.16 ± 0.1 (summer)	Tagged by NO_x emitted over Asia; standard deviations over time; other seasons are between spring and summer.
Emery et al. (2012); CAMx, GC boundary conditions (12 km^2)	Mar-Aug 2006; MDA8	Fires: *(10-50)*	Zero-out
Emmons et al. (2012);	2008; monthly mean	Asian: 1.5-4.2 (averaged over North America;	Tagged by NO_x emitted over

MOZART-4		minimum in August, maximum in April)	Asia
Lin et al. (2012a); GFDL AM3 (~50km^2)	Apr-Jun 2010; MDA8	Strat[e]: 15 western U.S. high-altitude sites 22±12 (mean) (*15-25 for observed O_3 at 60-70; 17-40 for observed O_3 at 70-85).* Median, bias-corrected[f]: 10-22 (west), 8-13 (northeast), 3-8 (southeast) (*maximum bias-corrected[f] 35-55 western U.S.; 30-45 eastern U.S.)*	Tagged using e90 tropopause
Lin et al. (2012b); GFDL AM3 (~50km^2)	May-Jun 2010; MDA8	Asian: *(8-15 Intermountain West when observed exceeds 60 ppb, June 20-22; 5-8 southern CA, when observed exceeds 75 ppb, June 22)*	Zero-out
Huang et al. (2013); STEM (60x60 km^2)	Jun-Jul 2008; MDA8, W126	Fires[g]: *(up to 18 ppb MDA8 and 9 ppm-h W126, highest over northern CA).* Biogenic[g]: *(up to 15 ppb MDA8 and 6–8 ppm-h W126 over northern CA and the Central Valley)*	—
Lapina et al. (2014); GC (2°x2.5°), AM3 (c48; ~200x200 km^2), STEM (60x60 km^2)	May-Jul 2010; daytime O_3, W126	W126 NAB: NO_x (80%), CO (10%), VOC (10%), and of this NO_x anthropogenic (14.5%), biomass burning (4.3%), soil (28.2%, 7% from outside U.S.), lightning (52.9, 40% from outside U.S.)	—
Pfister et al. (2013); WRF-Chem	June-July 2008; afternoon O_3	Tagging inflow to CA domain: 10 ± 9 ppb (20 ± 21% of total O_3) *(>8% to 8 h O_3> 75 ppb in 10% of cases; >13% in 1% of the cases; >12% to 8h O_3 > 65 ppb in 10% of cases; >21% in 1% of cases)*	Tagging of CO and NO_x
Zhang et al. (2014); GC (½°x⅔°)	Mar-Aug 2006; MDA8	Lightning: 6-10 ppb (summer). Fires: 1-3 (western U.S. summer mean) *(~20 local events).* Strat: 8-10 (western U.S. spring mean) *(up to 15)*	Zero-out except for stratosphere, which is tagged by stratospheric production
Lin et al. (2015); GFDL AM3 (c48; ~200x200 km^2)	Apr-May 1990-2012; average MDA8	Strat: western U.S. Apr-May 12-25 mean *(40-55 for observed O_3 > 65)*; western U.S. Jul-Aug 2-5 mean	Defined with a stratospheric O_3 tracer[e] and bias-corrected[f]
Murray et al. (2016); GC (2°x2.5°) plus ranges from published studies using GC or CMAQ	2004-2012; annual mean	Lightning: 1-4 (annual mean 2004-2012 GC), up to 6 local summer or monthly means, up to 10 local summer mean *(up to 46 local MDA8 in summer)*	GC values from Fig. 5 (Murray et al., 2016); other values are ranges across studies reported in Table 2 (Murray et al., 2016)
Huang et al. (2017); 8 global models, 1 regional model using 3 sets of boundary conditions	2010; monthly average, and May-June MDA8	North America response to 20% decrease in foreign (all non-North America, Europe, East Asia, and South Asia) anthropogenic emissions: 0.38-2.46 for all non-North American monthly average O_3; 0.24-	MDA8 response generally higher in May than June; MDA8 response smaller at CASTNET sites than

		0.34 for East Asian monthly average O_3; 0.35-0.58 for East Asian MDA8; monthly average O_3 response highest in Jan.	throughout the domain, and smaller on high O_3 days than all days
Nopmongcol et al. (2017); CAMx /C-IFS	2010	Contributions to summer average MDA8 from boundary conditions in 22 major cities: 20-40. Contributions from East Asia -20% emissions to western summer average MDA8 O_3: <1 in spring and <0.5 other seasons	—

[a]Table is adapted and updated from Fiore et al. (2014) and focuses on work since the McDonald-Buller (2011) review. See Section 4 in main paper.
[b]All are estimated by zeroing out named source unless explained otherwise.
[c]References within this work include a comparison of Zhang et al. (2011) to earlier work.
[d]GC: GEOS-Chem.
[e]Diagnosed with a tracer that is set to the O_3 mole fraction in the stratosphere according to the e90 definition of the tropopause (Prather et al., 2011) and then undergoes the chemical and depositional losses acting on the full O_3 tracer in the troposphere; see Lin et al. (2012a, 2015) for details.
[f]At sites where AM3 overestimates the observed MDA8 O_3 level and the estimated stratospheric contribution exceeds the model bias, this bias is assumed to be caused entirely by the stratospheric component.
[g]Estimated by extrapolating adjoint sensitivities and bias-correcting according to evaluation of base simulation with observations.

Supplementary Note 1. Observed ozone trends upwind of the western U.S.

The baseline ozone (O_3) that impacts the western U.S. represents complex O_3 production and loss processes that occur across the North Pacific Ocean and Asia, and even as far away as Europe and North America. (See Section 5 in main paper.) Since the 1990s O_3 precursor emissions have shifted from North America and Europe to East and South Asia, coupled with an equatorward shift, which increases O_3 production efficiency (Granier et al., 2011; Zhang et al., 2016). As a result, O_3 production has increased across East Asia at the surface and in the free troposphere (Cooper et al., 2014, Lin et al., 2017; Wang et al., 2017). Several recent studies show that O_3 has continued to increase in China. Sun et al. (2016) report changes of $+0.28 \pm 0.17$ ppb yr^{-1} (1994-2013) at Mt. Waliguan, on the Tibetan Plateau in central China and 1-2 ppb yr^{-1} (2003-2015) during summer at Mt. Tai, 1.5 km above the North China Plain. Ma et al. (2016) report an increase of ~1.1 ppb yr^{-1} (2003-2014) at Shangdianzi, a low elevation rural station northeast of Beijing (Ma et al., 2016). More broadly, commercial aircraft profiles above three regions of South and East Asia clearly demonstrate O_3 increases at the surface and in the free troposphere from 1994-2004 to 2005-2014 (Zhang et al., 2016). Finally, a recent analysis of all available surface O_3 monitors across Hong Kong, Taiwan, South Korea and Japan (data provided by the

Tropospheric Ozone Assessment Report [Schultz et al., 2017]), shows O_3 increased regionally from 2000 to 2014 at the rate of 0.45 ppb yr^{-1} for East Asia and 0.20 ppb yr^{-1} for Southeast Asia (Chang et al., 2017).

Between Asia and North America, Mauna Loa Observatory (MLO), Hawaii, is the only long-term monitoring site with information on O_3 trends above the marine boundary layer. While only partially upwind of mid-latitude North America, a new analysis of the dry air masses at MLO shows a strong increase of 0.42 ± 0.22 ppb yr^{-1} for 2000-2016 (Ziemke and Cooper, 2017). The dry air masses at this site have a mid-latitude origin and therefore are representative of the mid-latitude air masses that are transported across the North Pacific Ocean towards western North America.

Supplementary Note 2. Observed ozone trends along the U.S. northern and southern borders

The Tropospheric Ozone Assessment Report (TOAR) has provided trend analysis at all available rural O3 monitoring sites in Canada, the U.S., and Mexico (Schultz et al., 2017; Gaudel et al., 2017). (See Section 5 in main paper.) We have chosen to use the spring (MAM) and summer (JJA) daytime average and 95th percentile O3 metrics for the period 2000-2014 to evaluate changes in O3 close to the northern and southern borders of the U.S. There were no rural sites in northern Mexico that could provide information on O3 that may be transported from Mexico into the southern U.S. However, the O_3 monitor in Big Bend National Park near the U.S.–Mexico border gives some indication of O_3 trends in this region. Figure S1 shows that the annual 4th highest MDA8 O_3 value has increased significantly since 2000. This site also shows a significant increase of daytime average and 95th percentile O_3 in spring, but not in summer. Further investigation with an atmospheric chemistry model is required to determine the cause of this observed springtime O_3 increase at Big Bend.

In contrast, there are approximately three dozen Canadian rural monitoring sites close to the U.S. northern border. During spring, only one site (in British Columbia) had a significant positive O_3 trend (p-value < 0.05) and two sites (in Alberta) had significant decreases. The remaining sites show no significant trend. During summer, approximately 1/3 of the Canadian sites showed significant O_3 decreases (p-value < 0.10), mainly in the east, and no site showed a significant increase. When using the 95th percentile, the TOAR data show only two sites with significantly decreasing (p-value < 0.05) O_3 in spring (no site shows an increase), and roughly half of sites (mainly in the east) show significantly decreasing (p-value < 0.10) O_3 in summer (no site shows an increase).

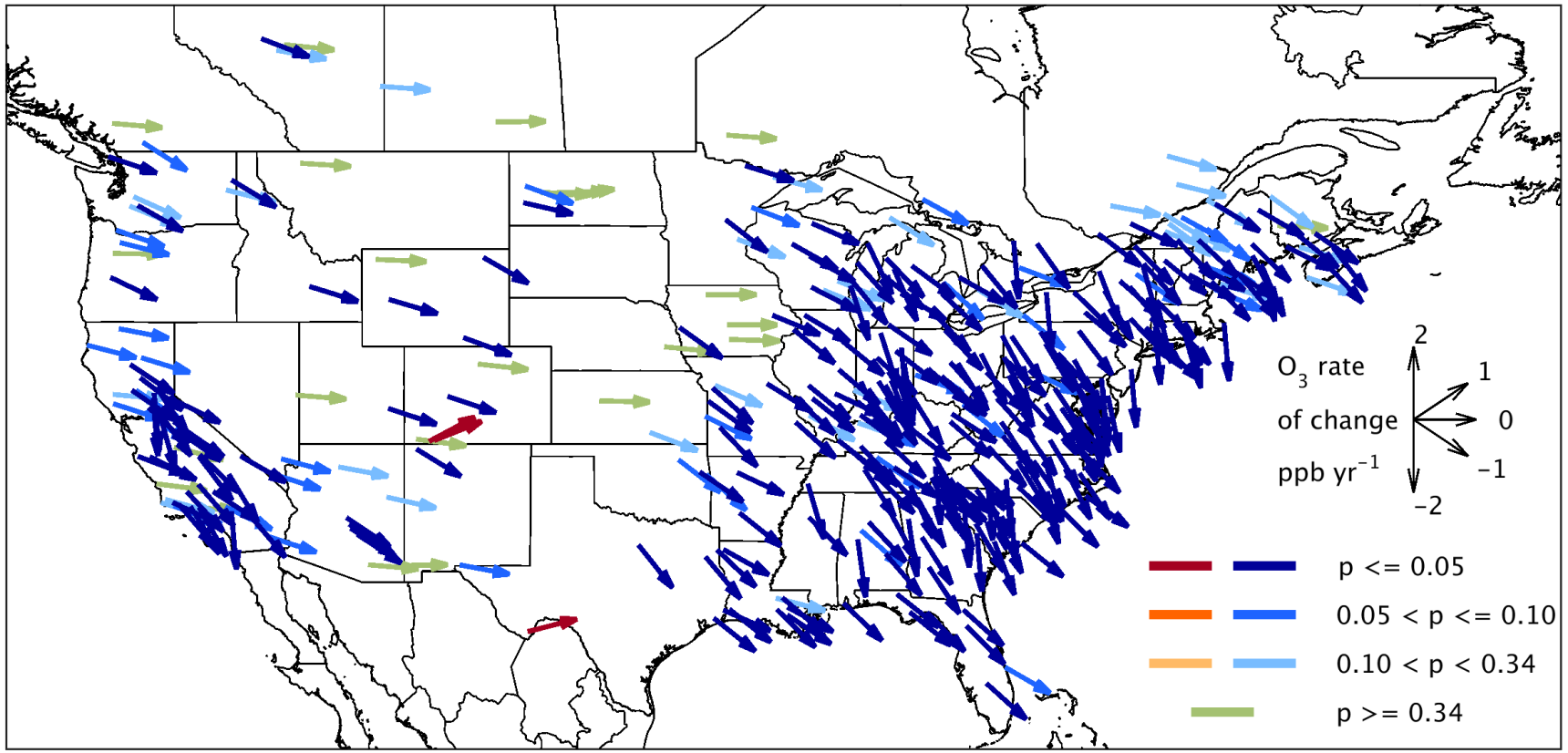

Figure S1. Trends in annual 4th highest MDA8 O_3 at rural sites in the U.S. and Canada.

Observations are April-September, 2000-2014. Vector colors indicate the p-values on the linear trend for each site: Blues indicate negative trends, oranges indicate positive trends, and green indicates weak or no trend; lower p-values have greater color saturation. Figure provided by the Tropospheric Ozone Assessment Report (Schultz et al., 2017). See Section 5 in main paper.

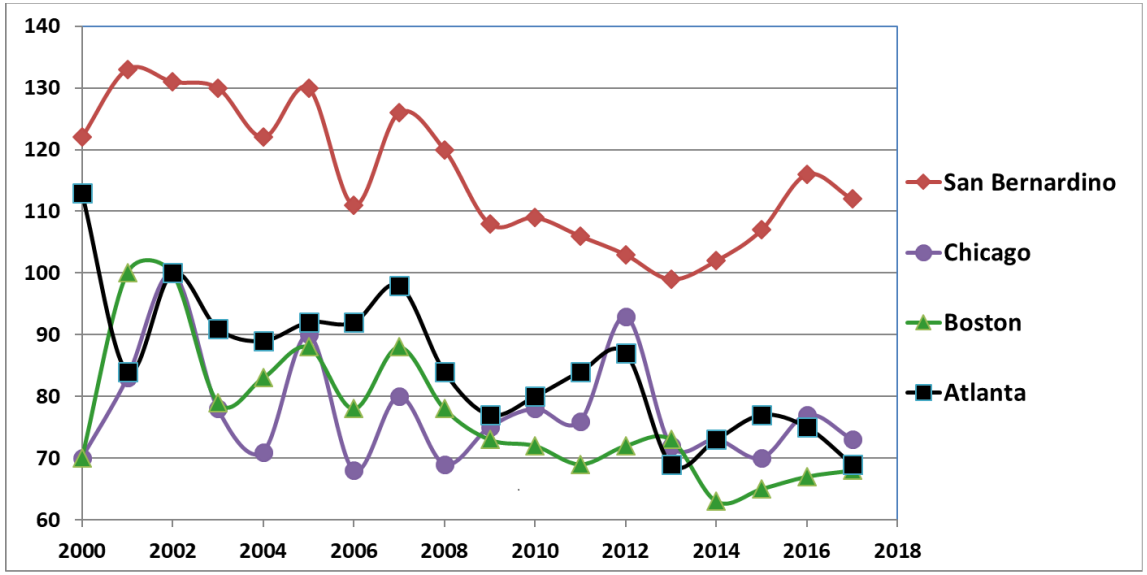
140
130
120
110
100
90
80
70
60
2000
2002
2004
2006
2008
2010
2012
2014
2016
2018
San Bernardino
Chicago
Boston
Atlanta

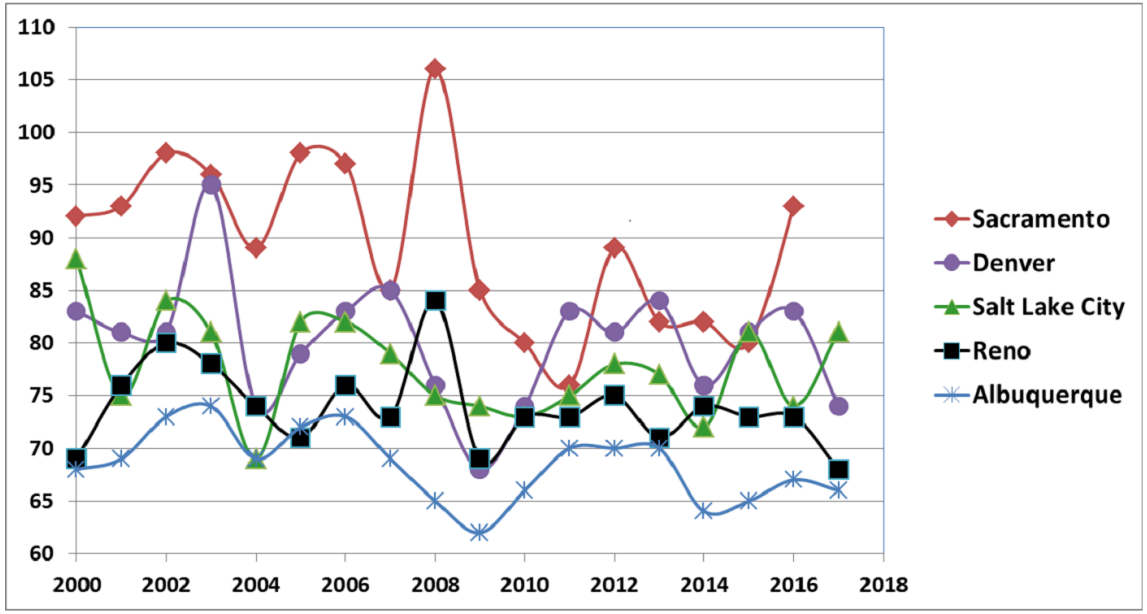
110
105
100
95
90
85
80
75
70
65
60
2000
2002
2004
2006
2008
2010
2012
2014
2016
2018
Sacramento
Denver
Salt Lake City
Reno
Albuquerque

Figure S2. Annual 4th highest MDA8 O_3 (ppb) for one site in each urban area.

The AQS ID numbers are given in Table S3. Data shown include any exceptional event days that may have been excluded from the O_3 design value calculation. See Section 5 in main paper.

Table S3. Linear trends and t-test results comparing 2000-2017 4th highest annual MDA8 values in 9 representative urban areas[a]

AQS	MSA[b]	Slope (ppb yr-1)	R^{2c}	T-test P value[d]	Altitude (meters asl)
06-071-0005	San Bernardino, CA	-1.58	0.58	<0.01	1384
17-097-1007	Chicago, IL	-0.43	0.07	0.57	178
13-121-0055	Atlanta, GA	-1.75	0.66	<0.01	292
25-009-2006	Boston, MA	-1.51	0.53	<0.01	52
35-001-0023	Albuquerque, NM	-0.32	0.26	0.020	1593
06-017-0010	Sacramento, CA	-0.86	0.28	0.001	585
49-035-3006	Salt Lake City, UT	-0.29	0.10	0.148	1306
08-059-0011	Denver, CO	-0.28	0.06	0.196	1832
32-031-0016	Reno, NV	-0.23	0.10	0.055	1306

[a]Data period covers January 1, 2000, to August 31, 2017, except for Sacramento, which ends at December 31, 2016. These data include any exceptional event days that may have been excluded from the O_3 design value (ODV) calculation. See Section 5 in main paper.
[b]For each metropolitan statistical area (MSA), we have chosen one site that is among the highest ODVs for that region and has a near complete data record going back to the year 2000.
[c]R^2 values greater than 0.22 are statistically significant ($P<0.05$).
[d]The t-test compares the 4th highest MDA8 values for the first half of this time period (2000-2008) with those for the second half (2009-2017).

Supplementary Note 3. EPA and WAQS modeling platforms

The EPA modeling is described in detail in the "Air Quality Modeling Technical Support Document for the 2015 Ozone NAAQS Preliminary Interstate Transport Assessment" (US EPA, 2016a). (See Section 6 in main paper.) The simulation applies the Comprehensive Air quality Model with extensions (CAMx version 6.32) to a continental U.S. domain at 12-km horizontal resolution. Meteorology inputs were developed using the Weather Research and Forecasting (WRF v3.4) and processed through pre-processing tools to 25 layers with approximately 19-meter resolution at the surface with coarser resolution aloft. The meteorological inputs and evaluation are described in the "Meteorological Model Performance for Annual 2011 WRF v3.4 Simulation" (US EPA, 2014b). The 2011 emissions are described in the "Technical Support Document (TSD) Preparation of Emissions Inventories for the Version 6.3, 2011 Emissions Modeling Platform" (US EPA, 2016b). Lateral

boundary conditions were developed using GEOS-Chem, extending the approach by Henderson et al. (2014) to the 2011 year. The CAMx Ozone Source Apportionment Technology (OSAT) was applied for the period from May 1 to September 29, which is the focus of this analysis. OSAT estimated biogenic, wildfire, boundary condition and within domain international contributions. The model performance at all sites is discussed in detail in Appendix A of the TSD (US EPA, 2016b).

The Western Air Quality Study (WAQS) modeling is described in detail in the WAQS 2011b Modeling Platform section of the Intermountain West Data Warehouse (IWDW, http://views.cira.colostate.edu/tsdw/) (WAQS, 2017). The 3-State Air Quality Study (3SAQS, predecessor to the WAQS) project performed photochemical grid modeling (PGM) for the year 2011 using the Comprehensive Air Quality Model with Extensions (CAMx) version 6.20 (http://www.camx.com/) and the Community Multiscale Air Quality (CMAQ) model version 5.0.2 (http://www.cmaq-model.org/).The 3SAQS 2011 Modeling Protocol (http://vibe.cira.colostate.edu/wiki/Attachments/Modeling/3SAQS_2011_Modeling_Protocol_Finalv2.pdf) details the CAMx and CMAQ configurations and justification for why they were chosen for the WAQS. Version B of the WAQS base 2011 modeling platform (WAQS_Base11b) includes air quality modeling results for 36-km, 12-km, and 4-km modeling domains (http://vibe.cira.colostate.edu/wiki/Attachments/Images/3SAQS_CAMx_Domains.png). The WAQS 2011b modeling platform includes a future projection year (2025) and CAMx source apportionment studies. The set-up and configuration of the WAQS 2011b platform was derived from the 3SAQS 2011 version A (3SAQS_CAMx_Base11a) modeling platform, but differs significantly in the input data used in the simulation. The link to the 2011b Modeling Platform Description (http://views.cira.colostate.edu/tsdw/DataRequest/PlatformBrowser.aspx?Platform=WAQS%202011b) provides a detailed description of the WAQS 2011b modeling platform.

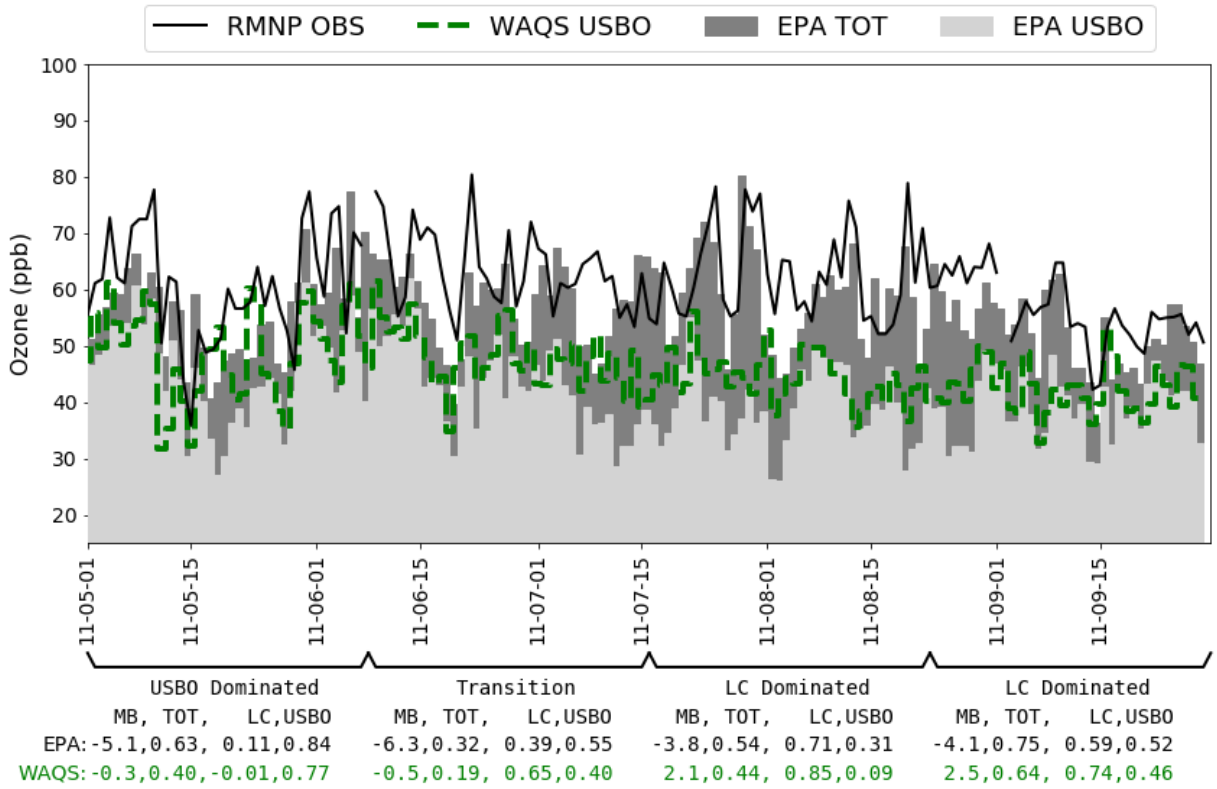

Figure S3. Observed and modeled MDA8 O_3 for Rocky Mountain National Park (RMNP) monitor.

Observed (black line) and modeled MDA8 O_3 (EPA model, top of dark grey) with USB O_3 contributions from EPA model (top of light grey) and WAQS model (dashed green line) for the RMNP monitor. For four simulation segments, the values below the axis for both models give the mean bias (MB), correlation (r) of total prediction with observations (TOT), correlation of local contribution with observations (LC), and correlation of USB O_3 contribution with observations (USBO). See Section 6 in main paper.

Table S4. Correlation matrix for O_3 observations (OBS), predictions (Mod), and contributions at Chatfield[a]

			EPA				WAQS			
		OBS	Mod	LC[b]	USBO	BC[c]	Mod	LC	USBO	BC
	OBS	1.00								
	Mod	0.73	1.00							
	LC	0.53	0.67	1.00						
	USBO	0.29	0.49	-0.33	1.00					
EPA	BC	0.22	0.37	-0.43	0.98	1.00				
	Mod	0.55	0.66	0.65	0.07	-0.05	1.00			
	LC	0.35	0.38	0.79	-0.44	-0.54	0.68	1.00		
	USBO	0.26	0.35	-0.18	0.65	0.61	0.41	-0.39	1.00	
WAQS	BC	0.15	0.24	-0.34	0.70	0.72	0.19	-0.57	0.95	1.00

[a]See Section 6 in main paper.
[b]LC: local contribution = Mod – USBO.
[c]BC: boundary conditions.

Supplementary Note 4. Rationale for excluding stratospheric intrusion days in analysis

June 7th was flagged by Colorado state as a stratospheric intrusion and June 24th was characteristic of an intrusion (e.g., atypical, early season, highly local) with hourly mole fractions over 100 ppb for four hours. (See Section 6 in main paper.) These simulations get most of their stratospheric contribution through the lateral boundary conditions including lower stratosphere (from the surface to 50 hPa) and O_3 mixed down outside the domain. Strong local intrusion events, however, may occur completely within the modeling domain and can be better simulated with a prescribed or parameterized (Xing et al., 2016) top condition. Observed or simulated days that are strongly influenced by stratospheric O_3 (e.g., stratospheric intrusions) are typically removed from attainment demonstration modeling applications as those events do not represent the source-receptor relationships of interest in an attainment demonstration (US EPA, 2014a).

Supplementary references

Brown-Steiner B, Hess P. 2011. Asian influence on surface ozone in the United States: A comparison of chemistry, seasonality, and transport mechanisms. *J Geophys Res* **116**: D17309. DOI: 10.1029/2011jd015846.

Chang K-L, Petropavlovskikh I, Cooper OR, Schultz MG, Wang T. 2017. Regional trend analysis of surface ozone observations from monitoring networks in eastern North America, Europe and East Asia. *Elementa* **5**(50). DOI: 10.1525/elementa.243.

Cooper OR, Parrish DD, Ziemke J, Balashov NV, Cupeiro M, et al. 2014. Global distribution and trends of tropospheric ozone: An observation-based review. *Elementa* **2**(29). DOI: 10.12952/journal.elementa.000029.

Dolwick P, Akhtar F, Baker KR, Possiel N, Simon H, et al. 2015. Comparison of background ozone estimates over the western United States based on two separate model methodologies. *Atmos Environ* **109**: 282–296. DOI: 10.1016/j.atmosenv.2015.01.005.

Dunker AM, Koo B, Yarwood G. 2017. Contributions of foreign, domestic and natural emissions to US ozone estimated using the path-integral method in CAMx nested within GEOS-Chem. *Atmos Chem Phys* **17**(20): 12553–12571. DOI: 10.5194/acp-17-12553-2017.

Emery C, Jung J, Downey N, Johnson J, Jimenez M, et al. 2012. Regional and global modeling estimates of policy relevant background ozone over the United States. *Atmos Environ* **47**: 206–217. DOI: 10.1016/j.atmosenv.2011.11.012.

Emmons LK, Hess PG, Lamarque JF, Pfister GG. 2012. Tagged ozone mechanism for MOZART-4, CAM-chem and other chemical transport models. *Geosci Model Dev* **5**(6): 1531–1542. DOI: 10.5194/gmd-5-1531-2012.

Fiore AM, Oberman JT, Lin MY, Zhang L, Clifton OE, et al. 2014. Estimating North American background ozone in U.S. surface air with two independent global models: Variability, uncertainties, and recommendations. *Atmos Environ* **96**: 284–300. DOI: 10.1016/j.atmosenv.2014.07.045.

Gaudel A, Cooper OR, et al. 2017. Tropospheric Ozone Assessment Report: Present-day ozone distribution and trends relevant to climate and global model evaluation. *Elementa.* **In review**.

Granier C, Bessagnet B, Bond T, D'Angiola A, van der Gon HD, et al. 2011. Evolution of anthropogenic and biomass burning emissions of air pollutants at global and regional scales during the 1980-2010 period. *Clim Change* **109**(1-2): 163–190. DOI: 10.1007/s10584-011-0154-1.

Henderson BH, Akhtar F, Pye HOT, Napelenok SL, Hutzell WT. 2014. A database and tool for boundary conditions for regional air quality modeling: description and evaluation. *Geosci Model Dev* **7**(1): 339–360. DOI: 10.5194/gmd-7-339-2014.

Huang M, Carmichael GR, Chai T, Pierce RB, Oltmans SJ, et al. 2013. Impacts of transported background pollutants on summertime western US air quality: model evaluation, sensitivity analysis and data assimilation. *Atmos Chem Phys* **13**(1): 359–391. DOI: 10.5194/acp-13-359-2013.

Huang M, Bowman KW, Carmichael GR, Lee M, Chai TF, et al. 2015. Improved western US background ozone estimates via constraining nonlocal and local source contributions using Aura TES and OMI observations. *J Geophys Res Atmos* **120**(8): 3572–3592. DOI: 10.1002/2014jd022993.

Huang M, Carmichael GR, Pierce RB, Jo DS, Park RJ, et al. 2017. Impact of intercontinental pollution transport on North American ozone air pollution: an HTAP phase 2 multi-model study. *Atmos Chem Phys* **17**(9): 5721–5750. DOI: 10.5194/acp-17-5721-2017.

Lapina K, Henze DK, Milford JB, Huang M, Lin MY, et al. 2014. Assessment of source contributions to seasonal vegetative exposure to ozone in the US. *J Geophys Res Atmos* **119**(1): 324–340. DOI: 10.1002/2013jd020905.

Lefohn AS, Emery C, Shadwick D, Wernli H, Jung J, et al. 2014. Estimates of background surface ozone concentrations in the United States based on model-derived source apportionment. *Atmos Environ* **84**: 275–288. DOI: 10.1016/j.atmosenv.2013.11.033.

Lin M, Fiore AM, Cooper OR, Horowitz LW, Langford AO, et al. 2012a. Springtime high surface ozone events over the western United States: Quantifying the role of stratospheric intrusions. *J Geophys Res Atmos* **117**(D00V22). DOI: 10.1029/2012jd018151.

Lin M, Fiore AM, Horowitz LW, Cooper OR, Naik V, et al. 2012b. Transport of Asian ozone pollution into surface air over the western United States in spring. *J Geophys Res Atmos* **117**(D00V07). DOI: 10.1029/2011JD016961.

Lin MY, Horowitz LW, Cooper OR, Tarasick D, Conley S, et al. 2015. Revisiting the evidence of increasing springtime ozone mixing ratios in the free troposphere over western North America. *Geophys Res Lett* **42**(20): 8719–8728. DOI: 10.1002/2015gl065311.

Lin M, Horowitz LW, Payton R, Fiore AM, Tonnesen GS. 2017. US surface ozone trends and extremes from 1980 to 2014: quantifying the roles of rising Asian emissions, domestic controls, wildfires, and climate *Atmos Chem Phys* **17**: 2943–2970. DOI: 10.5194/acp-17-2943-2017.

Ma ZQ, Xu J, Quan WJ, Zhang ZY, Lin WL, et al. 2016. Significant increase of surface ozone at a rural site, north of eastern China. *Atmos Chem Phys* **16**(6): 3969–3977. DOI: 10.5194/acp-16-3969-2016.

McDonald-Buller EC, Allen DT, Brown N, Jacob DJ, Jaffe DA, et al. 2011. Establishing policy relevant background (PRB) ozone concentrations in the United States. *Environ Sci Technol* **45**(22): 9484–9497. DOI: 10.1021/es2022818.

Mueller SF, Mallard JW. 2011. Contributions of Natural Emissions to Ozone and PM2.5 as Simulated by the Community Multiscale Air Quality (CMAQ) Model. *Environ Sci Technol* **45**(11): 4817–4823. DOI: 10.1021/es103645m. Corrected in *Environ Sci Technol* **45**: 7950. DOI: 10.1021/es2027086.

Murray LT. 2016. Lightning NO x and Impacts on Air Quality. *Current Pollution Reports* **2**(2): 115–133. DOI: 10.1007/s40726-016-0031-7.

Nopmongcol U, Jung J, Kumar N, Yarwood G. 2016. Changes in US background ozone due to global anthropogenic emissions from 1970 to 2020. *Atmos Environ* **140**: 446–455. DOI: 10.1016/j.atmosenv.2016.06.026.

Nopmongcol U, Liu Z, Stoeckenius T, Yarwood G. 2017. Modeling intercontinental transport of ozone in North America with CAMx for the Air Quality Model Evaluation International Initiative (AQMEII) Phase 3. *Atmos Chem Phys* **17**(16): 9931–9943. DOI: 10.5194/acp-17-9931-2017.

Pfister GG, Walters S, Emmons LK, Edwards DP, Avise J. 2013. Quantifying the contribution of inflow on surface ozone over California during summer 2008. *J Geophys Res Atmos* **118**(21): 12282–12299. DOI: 10.1002/2013jd020336.

Prather MJ, Zhu X, Tang Q, Hsu JN, Neu JL. 2011. An atmospheric chemist in search of the tropopause. *J Geophys Res Atmos* **116**(D04306). DOI: 10.1029/2010jd014939.

Schultz MG, Schröder S, Lyapina O, Cooper O, Galbally I, et al. 2017. Tropospheric Ozone Assessment Report: Database and Metrics Data of Global Surface Ozone Observations. *Elementa* **5**(58). DOI: 10.1525/elementa.244.

Sun L, Xue LK, Wang T, Gao J, Ding AJ, et al. 2016. Significant increase of summertime ozone at Mount Tai in Central Eastern China. *Atmos Chem Phys* **16**(16): 10637–10650. DOI: 10.5194/acp-16-10637-2016.

U.S. Environmental Protection Agency (US EPA). 2014a. Draft Modeling Guidance for Demonstrating Attainment of Air Quality Goals for Ozone, $PM_{2.5}$, and Regional Haze. Research Triangle Park, NC: U.S. Environmental Protection Agency, Office of Air Quality Planning and Standards. Available at https://www3.epa.gov/scram001/guidance/guide/Draft_O3-PM-RH_Modeling_Guidance-2014.pdf. Accessed October 27, 2017.

U.S. Environmental Protection Agency (US EPA). 2014b. Meteorological Model Performance for Annual 2011 WRF v3.4 Simulation. Office of Air Quality Planning and Standards. Available at https://www3.epa.gov/ttn/scram/reports/MET_TSD_2011_final_11-26-14.pdf. Accessed October 27, 2017.

U.S. Environmental Protection Agency (US EPA). 2016a. Air Quality Modeling Technical Support Document for the 2015 Ozone NAAQS Preliminary Interstate Transport Assessment. Research Triangle Park, NC: U.S. Environmental Protection Agency, Office of Air Quality Planning and Standards. Available at https://www.epa.gov/sites/production/files/2017-01/documents/aq_modeling_tsd_2015_o3_naaqs_preliminary_interstate_transport_assessmen.pdf. Accessed October 27, 2017.

U.S. Environmental Protection Agency (US EPA). 2016b. Technical Support Document (TSD) Preparation of Emissions Inventories for the Version 6.3, 2011 Emissions Modeling Platform. Research Triangle Park, NC: U.S. Environmental Protection Agency, Office of Air and Radiation, Office of Air Quality Planning and Standards. Available at https://www.epa.gov/sites/production/files/2016-09/documents/2011v6_3_2017_emismod_tsd_aug2016_final.pdf. Accessed October 27, 2017.

Wang T, Xue LK, Brimblecombe P, Lam YF, Li L, et al. 2017. Ozone pollution in China: A review of concentrations, meteorological influences, chemical precursors, and effects. *Sci Total Environ* **575**: 1582–1596. DOI: 10.1016/j.scitotenv.2016.10.081.

Western Air Quality Study (WAQS). 2017. Western Air Quality 2011b Modeling Platform. Available at http://vibe.cira.colostate.edu/wiki/wiki/%209166/waqs-2011b-modeling-platform. Accessed November 7, 2017.

Wild O, Fiore AM, Shindell DT, Doherty RM, Collins WJ, et al. 2012. Modelling future changes in surface ozone: a parameterized approach. *Atmos Chem Phys* **12**(4): 2037–2054. DOI: 10.5194/acp-12-2037-2012.

Xing J, Mathur R, Pleim J, Hogrefe C, Wang JD, et al. 2016. Representing the effects of stratosphere-troposphere exchange on 3-D O-3 distributions in chemistry transport models using a potential vorticity-based parameterization. *Atmos Chem Phys* **16**(17): 10865–10877. DOI: 10.5194/acp-16-10865-2016.

Zhang L, Jacob DJ, Downey NV, Wood DA, Blewitt D, et al. 2011. Improved estimate of the policy-relevant background ozone in the United States using the GEOS-Chem global model with 1/2 degrees x 2/3 degrees horizontal resolution over North America. *Atmos Environ* **45**(37): 6769–6776. DOI: 10.1016/j.atmosenv.2011.07.054.

Zhang L, Jacob DJ, Yue X, Downey NV, Wood DA, et al. 2014. Sources contributing to background surface ozone in the US Intermountain West. *Atmos Chem Phys* **14**(11): 5295–5309. DOI: 10.5194/acp-14-5295-2014.

Zhang YQ, Cooper OR, Gaudel A, Thompson AM, Nedelec P, et al. 2016. Tropospheric ozone change from 1980 to 2010 dominated by equatorward redistribution of emissions. *Nat Geosci* **9**(12): 875–879. DOI: 10.1038/ngeo2827.

Ziemke JR, Cooper OR. 2017. Tropospheric ozone [in "State of the Climate in 2016"]. *Bull Am Meteorol Soc* **98(**8): S52–S54. DOI: 10.1175/2017BAMSStateoftheClimate.1.

Supplementary acknowledgements

We thank the Tropospheric Ozone Assessment Report (TOAR) initiative for providing Figures S1 and S2, depicting the present-day (2010-2014) distribution and trends (2000-2014) of the annual 4th highest maximum daily 8-hr average O_3 value at all available rural monitoring sites across the U.S. and southern Canada (Schultz et al., 2017). These and similar plots, along with the underlying O_3 metrics, can be downloaded from: Schultz, MG, et al., Tropospheric Ozone Assessment Report, links to Global surface O_3 datasets, https://doi.pangaea.de/10.1594/PANGAEA.876108.

Figure Legends

Figure S1. Trends in annual 4th highest MDA8 O_3 at rural sites in the U.S. and Canada.
Observations are April-September, 2000-2014. Vector colors indicate the p-values on the linear trend for each site: Blues indicate negative trends, oranges indicate positive trends, and green indicates weak or no trend; lower p-values have greater color saturation. Figure provided by the Tropospheric Ozone Assessment Report (Schultz et al., 2017). See Section 5 in main paper.

Figure S2. Annual 4th highest MDA8 O_3 for one site in each urban area.
The AQS ID numbers are given in Table S3 below. Data shown include any exceptional event days that may have been excluded from the O_3 design value calculation. See Section 5 in main paper.

Figure S3. Observed and modeled MDA8 O_3 for Rocky Mountain National Park (RMNP) monitor.

Observed (black line) and modeled MDA8 O_3 (EPA model, top of dark grey) with USB O_3 contributions from EPA model (top of light grey) and WAQS model (dashed green line) for the RMNP monitor. For four simulation segments, the values below the axis for both models give the mean bias (MB), correlation (r) of total prediction with observations (TOT), correlation of local contribution with observations (LC), and correlation of USB O_3 contribution with observations (USBO). See Section 6 in main paper.

Tables

Table S1. Model estimates for background ozone (O^3) (multiple definitions)[a]

Study; Model (horizontal resolution)	Study period; Metric	Background: Seasonal average values (ppb) *(High events)*	Approach/Notes
McDonald-Buller et al. (2011)[b], based on Zhang et al. (2011); GC[c] (½°x⅔°)	Mar-Aug 2006-2008; MDA8	NAB[d]: 39-44 (spring); 35-45 (summer); low-altitude 27±8; high-altitude 40±7 *(51-59, 4th highest)*	Zero-out
Emery et al. (2012); CAMx (12 km^2), GC boundary conditions	Mar-Aug 2006; MDA8	NAB: 25-50; 20-45 in GC (*35-100, 4th highest; 65 maximum without fires; 55 maximum in GC)*	Zero-out
Lin et al. (2012a); GFDL AM3 (~50km^2)	Apr-Jun 2010; MDA8	NAB: 15 western U.S. high-altitude sites 50±11 (*55±11, days when observed exceeds 60)*	Zero-out, bias corrected[e]
Huang et al. (2013); STEM (60x60 km^2)	Jun-Jul 2008; MDA8 & W126	Transported background: MDA8 30-35 EPA Regions 9 and 10; W126 10-17 ppm-h R9 & 3-4 ppm-h R10	Extrapolate adjoint sensitivities and bias-correct
Lapina et al. (2014); GC (2°x2.5°), AM3 (c48; ~200x200 km^2), and STEM (60x60 km^2)	May-Jul 2010; daytime O_3 & W126	NAB daytime O_3: multi-model spatial range of 18.3-41.6, US mean 56-67%, Intermountain West mean 64-78%; NAB W126: mostly < 3ppm hr, U.S.-wide mean 4-12%, <6 % in East, <35% in West	Zero-out

Dolwick et al. (2015); CMAQ, CAMx (12km^2)	Apr-Oct 2007; MDA8	USB[d] and USB[f]: Intermountain West 40-45, bias-corrected[g], seasonal mean; Pacific Coast 25-35 *(highest 10% of days in a season: >70-80%; western U.S. rural sites; >40-60%, western U.S. urban sites)*	Zero-out in CMAQ, source apportionment in CAMx
Fiore et al. (2014); GC (½°x⅔°)	Mar-Aug 2006; MDA8	NAB: western U.S. high-altitude sites ~40-50 (spring), ~25-40 (summer); eastern U.S. ~20-30 (summer)	Zero-out
Fiore et al. (2014); GFDL AM3 (2°x2°)	1981-2007 average	NAB:15-50, highest in western U.S. and in spring	Zero-out
Lefohn et al. (2014); GC/CAMx (12x12km^2)	2006	OSAT[f]-derived emissions-influenced background: *(can be >70% at high-elevation western U.S. sites)*	Source apportionment
Huang et al. (2015); GC (assimilated TES O_3)/STEM (assimilated OMI NO_2) (12×12 km^2)	Jun-Jul 2008; MDA8	USB[h]: Spatial range over CA and NV 35-65, domain mean of 48, 77% total	Zero-out within domain (CA and NV)
Lin et al. (2015); GFDL AM3 (c48; ~200x200 km^2)	1990-2012; MDA8	NAB over western U.S. Apr-May: 40-50 *(50-75 for observed O_3> 65)*; NAB over western U.S. Jul-Aug: 20	Zero-out
Dunker et al. (2017); CAMx /GC	March-Sep 2010; MDA8	USB[i] in 12 cities: (*ranges from 30.0 for Boston to 60.3 for Denver, and 42 for Boston to 64.8 for Denver, on 10 highest global background O_3 days)*	Path-integral method
Lin et al. (2017)[j]; GFDL AM3 (c48; ~200x200 km^2)	1980-2014; MDA8	Changes in western U.S. NAB from 1980s to 2000s: 6.3±1.9 (spring); 4.2±2.0 (summer)	Zero-out
Nopmongcol et al. (2016)[j]; CAMx /GC	1970-2020; 4th highest MDA8	USB: range increased from 40-55 to 45-60	Zero-out
Wild et al. (2012)[j]; 14 global models (1°x1° to 5°x5°)	1960-1990; annual mean	NAB: increased 0.67/decade, leveling off by 2000	Parameterization based on continental-average O_3 responses to 20% reductions in anthropogenic emissions

[a]Table is adapted and updated from Fiore et al. (2014) and focuses on work since the McDonald-Buller (2011) review. See Section 4 in main paper.

[b]References within this work include a comparison of Zhang et al. (2011) to earlier work.

[c]GC: GEOS-Chem.

[d]North American background (NAB) or U.S. background (USB), defined as the O_3 mole fractions sampled from the lowest (surface) model layer in a simulation with North American or U.S., respectively, anthropogenic emissions within the domain set to zero. Studies differ in their domain boundaries and also their treatments of fertilizer, shipping, agricultural waste burning and aircraft emissions.

[e]At sites where AM3 overestimates the observed MDA8 O_3 level, the bias is assumed to be caused entirely by excessive background.
[f]The Ozone Source Apportionment Technology (OSAT) in CAMx is designed to attribute O_3 formation to precursors tagged by source. When precursors come from multiple sources, O_3 is assigned to the source associated with the limiting chemical precursor (NO_x or VOC), which is identified based on an empirical threshold of radical termination pathways (i.e., if $P(H_2O_2)/P(HNO_3) > 0.35$ then NO_x, otherwise VOC).
[g]Bias-correction was calculated by taking the daily model calculated USB/Base MDA8 O_3 fractions and multiplying it by the daily MDA8 bias at each monitoring location. This product is then subtracted from the original USB[d] (zero-out) or USB[f] (source apportionment) estimate.
[h]Huang et al. (2015) zero-out anthropogenic emissions within the STEM domain (CA and NV) only so this estimate may include some O_3 produced from U.S. anthropogenic emissions that is transported through the boundary conditions.
[i]Calculated as Base – U.S. anthro columns of Table 3 (Dunker et al., 2017) for the base (T10Base) and high-background (T10Bkgd) days, which excludes a small (<0.5 ppb) anthropogenic contribution to the top boundary condition.
[j]This study looked at long-term O_3 trends.

Table S2. Model estimates for non-controllable ozone sources (NCOS)[a]

Study; Model (horizontal resolution)	Study period; Metric	Non-controllable ozone source (NCOS): Mean estimate (ppb)[b] *(Events)*	Approach/Notes
McDonald-Buller et al., 2011[c], based on Zhang et al. (2011); GC[d] (½°x⅔°)	Mar-Aug 2006-2008; MDA8	Natural: 18±6 (low altitude), 27±6 (high altitude) *(34-45, 4th highest).* CH_4+ICT: 13-16 (spring) 11-13 (summer), 13 (high altitude), 9 (low altitude)	Zero-out
Mueller and Mallard (2011); CMAQ, GC boundary conditions (36 km^2)	2002; MDA8	Fires: *(30-50 western U.S.)* Lightning: *(10-30 southern U.S.)*	Zero-out
Brown-Steiner and Hess (2011); CAM-Chem	2001-2005; seasonal means	Asian: western U.S. 3.36 ± 1.3 (spring), 1.36 ± 0.7 (summer); central U.S. 1.66 ± 0.5 (spring), 0.70 ± 0.3 (summer); eastern U.S. 0.56 ± 0.3 (spring), 0.16 ± 0.1 (summer)	Tagged by NO_x emitted over Asia; standard deviations over time; other seasons are between spring and summer.
Emery et al. (2012); CAMx, GC boundary conditions (12 km^2)	Mar-Aug 2006; MDA8	Fires: *(10-50)*	Zero-out
Emmons et al. (2012); MOZART-4	2008; monthly mean	Asian: 1.5-4.2 (averaged over North America; minimum in August, maximum in April)	Tagged by NO_x emitted over Asia
Lin et al. (2012a); GFDL AM3 (~50km^2)	Apr-Jun 2010; MDA8	Strat[e]: 15 western U.S. high-altitude sites 22±12 (mean) (*15-25 for observed O_3 at 60-70; 17-40 for observed O_3 at 70-85).* Median, bias-corrected[f]: 10-22 (west), 8-13 (northeast), 3-8 (southeast) (*maximum bias-corrected[f] 35-55 western U.S.; 30-45 eastern U.S.)*	Tagged using e90 tropopause
Lin et al. (2012b); GFDL AM3	May-Jun 2010;	Asian: *(8-15 Intermountain West when observed*	Zero-out

(~50km^2)	MDA8	*exceeds 60 ppb, June 20-22; 5-8 southern CA, when observed exceeds 75 ppb, June 22)*	
Huang et al. (2013); STEM (60x60 km^2)	Jun-Jul 2008; MDA8, W126	Fires[g]: *(up to 18 ppb MDA8 and 9 ppm-h W126, highest over northern CA).* Biogenic[g]: *(up to 15 ppb MDA8 and 6–8 ppm-h W126 over northern CA and the Central Valley)*	—
Lapina et al. (2014); GC (2°x2.5°), AM3 (c48; ~200x200 km^2), STEM (60x60 km^2)	May-Jul 2010; daytime O_3, W126	W126 NAB: NO_x (80%), CO (10%), VOC (10%), and of this NO_x anthropogenic (14.5%), biomass burning (4.3%), soil (28.2%, 7% from outside U.S.), lightning (52.9, 40% from outside U.S.)	—
Pfister et al. (2013); WRF-Chem	June-July 2008; afternoon O_3	Tagging inflow to CA domain: 10 ± 9 ppb (20 ± 21% of total O_3) *(>8% to 8 h O_3> 75 ppb in 10% of cases; >13% in 1% of the cases; >12% to 8h O_3 > 65 ppb in 10% of cases; >21% in 1% of cases)*	Tagging of CO and NO_x
Zhang et al. (2014); GC (½°x⅔°)	Mar-Aug 2006; MDA8	Lightning: 6-10 ppb (summer). Fires: 1-3 (western U.S. summer mean) *(~20 local events).* Strat: 8-10 (western U.S. spring mean) *(up to 15)*	Zero-out except for stratosphere, which is tagged by stratospheric production
Lin et al. (2015); GFDL AM3 (c48; ~200x200 km^2)	Apr-May 1990-2012; average MDA8	Strat: western U.S. Apr-May 12-25 mean *(40-55 for observed O_3 > 65)*; western U.S. Jul-Aug 2-5 mean	Defined with a stratospheric O_3 tracer[e] and bias-corrected[f]
Murray et al. (2016); GC (2°x2.5°) plus ranges from published studies using GC or CMAQ	2004-2012; annual mean	Lightning: 1-4 (annual mean 2004-2012 GC), up to 6 local summer or monthly means, up to 10 local summer mean *(up to 46 local MDA8 in summer)*	GC values from Fig. 5 (Murray et al., 2016); other values are ranges across studies reported in Table 2 (Murray et al., 2016)
Huang et al. (2017); 8 global models, 1 regional model using 3 sets of boundary conditions	2010; monthly average, and May-June MDA8	North America response to 20% decrease in foreign (all non-North America, Europe, East Asia, and South Asia) anthropogenic emissions: 0.38-2.46 for all non-North American monthly average O_3; 0.24-0.34 for East Asian monthly average O_3; 0.35-0.58 for East Asian MDA8; monthly average O_3 response highest in Jan.	MDA8 response generally higher in May than June; MDA8 response smaller at CASTNET sites than throughout the domain, and smaller on high O_3 days than all days
Nopmongcol et al. (2017); CAMx /C-IFS	2010	Contributions to summer average MDA8 from boundary conditions in 22 major cities: 20-40. Contributions from East Asia -20% emissions to western summer average MDA8 O_3: <1 in spring and <0.5 other seasons	—

[a]Table is adapted and updated from Fiore et al. (2014) and focuses on work since the McDonald-Buller (2011) review. See Section 4 in main paper.
[b]All are estimated by zeroing out named source unless explained otherwise.
[c]References within this work include a comparison of Zhang et al. (2011) to earlier work.
[d]GC: GEOS-Chem.
[e]Diagnosed with a tracer that is set to the O_3 mole fraction in the stratosphere according to the e90 definition of the tropopause (Prather et al., 2011) and then undergoes the chemical and depositional losses acting on the full O_3 tracer in the troposphere; see Lin et al. (2012a, 2015) for details.
[f]At sites where AM3 overestimates the observed MDA8 O_3 level and the estimated stratospheric contribution exceeds the model bias, this bias is assumed to be caused entirely by the stratospheric component.
[g]Estimated by extrapolating adjoint sensitivities and bias-correcting according to evaluation of base simulation with observations.

Table S3. Linear trends and t-test results comparing 2000-2017 4th highest annual MDA8 values in 9 representative urban areas[a]

AQS	MSA[b]	Slope (ppb yr-1)	R^{2c}	T-test P value[d]	Altitude (meters asl)
06-071-0005	San Bernardino, CA	-1.58	0.58	<0.01	1384
17-097-1007	Chicago, IL	-0.43	0.07	0.57	178
13-121-0055	Atlanta, GA	-1.75	0.66	<0.01	292
25-009-2006	Boston, MA	-1.51	0.53	<0.01	52
35-001-0023	Albuquerque, NM	-0.32	0.26	0.020	1593
06-017-0010	Sacramento, CA	-0.86	0.28	0.001	585
49-035-3006	Salt Lake City, UT	-0.29	0.10	0.148	1306
08-059-0011	Denver, CO	-0.28	0.06	0.196	1832
32-031-0016	Reno, NV	-0.23	0.10	0.055	1306

[a]Data period covers January 1, 2000, to August 31, 2017, except for Sacramento, which ends at December 31, 2016. These data include any exceptional event days that may have been excluded from the O_3 design value (ODV) calculation. See Section 5 in main paper.
[b]For each metropolitan statistical area (MSA), we have chosen one site that is among the highest ODVs for that region and has a near complete data record going back to the year 2000.
[c]R^2 values greater than 0.22 are statistically significant ($P<0.05$).
[d]The t-test compares the 4th highest MDA8 values for the first half of this time period (2000-2008) with those for the second half (2009-2017).

Table S4. Correlation matrix for O_3 observations (OBS), predictions (Mod), and contributions at Chatfield[a]

			EPA				WAQS			
		OBS	Mod	LC[b]	USBO	BC[c]	Mod	LC	USBO	BC
	OBS	1.00								
	Mod	0.73	1.00							
	LC	0.53	0.67	1.00						
	USBO	0.29	0.49	-0.33	1.00					
EPA	BC	0.22	0.37	-0.43	0.98	1.00				
	Mod	0.55	0.66	0.65	0.07	-0.05	1.00			
	LC	0.35	0.38	0.79	-0.44	-0.54	0.68	1.00		
	USBO	0.26	0.35	-0.18	0.65	0.61	0.41	-0.39	1.00	
WAQS	BC	0.15	0.24	-0.34	0.70	0.72	0.19	-0.57	0.95	1.00

[a]See Section 6 in main paper.
[b]LC: local contribution = Mod – USBO.
[c]BC: boundary conditions.